RSC Advances

COMMUNICATION

In situ reductive regeneration of zerovalent iron nanoparticles immobilized on cellulose for atom efficient Cr(VI) adsorption†

Cite this: *RSC Adv.*, 2015, **5**, 89441

Received 26th September 2015
Accepted 13th October 2015

DOI: 10.1039/c5ra19917d

www.rsc.org/advances

Archana Kumari Sharma,[a] Rabindra Kumar,[a] Sunil Mittal,[a] Shamima Hussain,[b] Meenu Arora,[c] Ramesh Chand Sharma[a] and J. Nagendra Babu*[d]

Zerovalent iron nanoparticles (nZVI) (11.8 ± 0.2% w/w) immobilized on microcrystalline cellulose (C-nZVI) were synthesized and studied for Cr(VI) sorption. The material showed good atom economy for Cr(VI) adsorption (562.8 mg g^{-1} of nZVI). Oxidation of cellulose to cellulose dialdehyde leads to *in situ* regeneration of nZVI which is responsible for the atom efficient Cr(VI) sorption by C-nZVI.

1. Introduction

In recent years, zerovalent iron (ZVI) material has evolved as a promising sorbent for the removal of various contaminants from soil and groundwater due to its redox properties and low cost.[1] Zerovalent iron with a size in nanoscale orders is known as nZVI. The nZVI has a high surface area which is responsible for its high reactivity.[2] nZVI has been reported to remove various pollutants like heavy metals,[3] halogenated organics,[4] nitrate[5] *etc.* from wastewater and contaminated soils by reduction or reductive adsorption. However, the use of nZVI in water treatment technologies is limited by its properties like magnetic behaviour induced agglomeration and oxidation based surface passivation. These properties lead to the loss of adsorption potential of nZVI.[6] Several stabilization or immobilization approaches have been explored to achieve enhanced stability and activity of nZVI.[7] Natural polysaccharide based stabilizers like starch,[8] chitin, chitosan,[9] alginates[10] and CMC[11] have been applied for this purpose. The hydroxyl and amine moieties of these polysaccharide derivatives stabilize the nZVI through hydrogen bonding. However, most of these stabilizers are either water soluble or susceptible to microbial degradation, which in turn destabilize and subsequently oxidize nZVI.

Cellulose is one of the most abundant sustainable natural polysaccharides on earth. It is found in cell wall of plants, bacteria, fungi and many other living forms. Its salient properties like biocompatibility, biodegradability, non-toxicity upon degradation, recalcitrance and regeneration makes it a sustainable polymer for various uses including cosmetics, veterinary, food, wood, paper, fibres, clothes, bio-refineries and pharmaceutical industries.[12] Recently, cellulose in different polymorphic and morphological forms have found its application as a stabilizer in number of metal nanoparticle synthesis.[13] He *et al.* reported *in situ* synthesis of Au, Ag, Pt and Pd nanoparticles in porous cellulose fibres.[14] Apart from the template effect of nanoporous structure, cellulose also features as reducing agent for the synthesis of metal nanoparticles like Pt, Ag and Au nanoparticles.

While the present work was under progress, few cellulose immobilized nZVI materials have been reported for adsorption studies.[15] Datta *et al.* reported nZVI immobilized on cellulose filter paper as a potential material for chromium sorption.[15a] Similarly, Zhou *et al.* synthesized magnetic cellulose nanocomposite with a loading of 30% w/w nZVI which showed good adsorption efficiency for arsenic (92.8 mg g^{-1}).[15b] Both the studies show efficient adsorption behaviour of nZVI immobilized on cellulose. However the studies were preliminary and explored the nanocavity of the cellulose immobilizer. Thus, in the present study, microcrystalline cellulose (MCC) immobilized nZVI (C-nZVI) were synthesized and studied for their reductive adsorption of Cr(VI). Surprisingly, high atom economy w.r.t. nZVI for Cr(VI) adsorption was observed with C-nZVI material. Upon further investigation an unusual *in situ* reductive adsorption by nZVI immobilized material was observed. The mechanism of Cr(VI) adsorption by C-nZVI has been proposed to involve the polyol system of cellulose.

2. Materials and methods

All chemicals used in the experiments were of analytical grade. Microcrystalline cellulose Avicel PH-101® was procured from

[a]*Centre for Environmental Science & Technology, School of Environment and Earth Sciences, Central University of Punjab, Bathinda-151 001, Punjab, India*
[b]*UGC-DAE Consortium for Scientific Research, Kalpakkam Node, Kokilamedu-603 104, Tamilnadu, India*
[c]*Department of Chemistry, Multani Mal Modi College, Patiala, 147 001, Punjab, India*
[d]*Centre for Chemical Sciences, School of Basic and Applied Sciences, Central University of Punjab, Bathinda-151 001, Punjab, India. E-mail: nagendra.rd@gmail.com*

† Electronic supplementary information (ESI) available. See DOI: 10.1039/c5ra19917d

Sigma-Aldrich (St. Louis, USA). Deionized water was used for preparation of all the reagents. Total chromium and Cr(VI) were determined using diphenylcarbazide method.[16] Iron in C-nZVI was analysed by phenanthroline method, upon HNO_3/H_2SO_4 digestion of the sample.[17]

2.1 Synthesis of microcrystalline cellulose immobilized zerovalent iron nanoparticle (C-nZVI)

MCC (3.50 g) was dissolved in 250 mL of deionized water for the synthesis of C-nZVI at room temperature. Upon dissolution, $FeCl_3$ (1.50 g) was added to reaction mixture with vigorous stirring. To this solution was added dropwise a 20% aqueous $NaBH_4$ solution (100 mL) at a rate of 1 mL min^{-1}. Upon subsequent addition of $NaBH_4$ solution, the reaction mixture turned black with foam formation. Excess of borohydride solution was added for complete reduction leading to the formation of suspended material. The black material was separated by filtration, washed with methanol and dried *in vacuo*.

2.2 Physical characterization of C-nZVI

Fourier Transformed Infra-Red (FTIR) spectra of Microcrystalline Cellulose (MCC), C-nZVI and chromium adsorbed C-nZVI, were recorded on a BRUKER TENSOR 27 instrument. Morphological characterization was obtained upon analysis of gold coated sample using Scanning Electron Microscope (SEM JSM-6610LV) and EDX using oxford. BET surface area experiment was carried out by Belsorp adsorption/desorption data analysis software under nitrogen environment using Micromeritics Inc. ASAP 2010 Surface Area Analyzer for the determination of pore diameter and surface area of the nZVI particle. Thermogravimetric analysis (TGA) was carried out at a heating rate of 10 °C min^{-1} upto 500 °C using a Shimadzu TG-60H TG analyzer under N_2 environment. X-ray diffraction (XRD) analysis was carried out using Pan analytical X'Pert-Pro model. X-ray photoelectron spectroscopy (XPS) measurement was performed using PHOBIOS HSA3500 DLSEGD analyzer with excitation energy of 1486.74 eV. CHN elemental analysis for C-nZVI, $FeCl_3$ treated C-nZVI, chromium adsorbed C-nZVI were carried out using Thermo Finningan elemental analyser.

2.3 Adsorption and kinetics for Cr(VI) adsorption by C-nZVI

Adsorption experiments were carried out by maintaining a 100 mL of Cr(VI) solution (1–10 mg L^{-1}) at pH 3. C-nZVI (10 mg) were added to the solutions and maintained under constant shaking at 25 ± 2 °C for 24 h.

For the kinetic study, 10 mg of C-nZVI were added to a 100 mL solution of 10 mg L^{-1} Cr(VI) solution. The sample was shaken at 25 ± 2 °C for 24 h. A small aliquot was drawn and analysed at various time interval. The concentration of Cr(VI) adsorbed was plotted as a function of time. The kinetic data was studied for its pseudo-first order and pseudo-second order kinetic behaviour.

3. Results and discussion

The material C-nZVI was synthesized by borohydride reduction of $FeCl_3$ dissolved in an aqueous suspension of MCC. The C-nZVI was analysed for its iron content[17] and revealed a loading of 11.8 ± 0.2% w/w iron onto the cellulose.

To investigate the morphology of the C-nZVI, SEM imaging was carried out (Fig. 1A). The images showed iron nanoparticles spread on the surface of cellulose with very poor adherence of particle to the polymer surface (Fig. 1A). The nZVI were in the size range of 50–60 nm, with chain like aggregation. The aggregation of iron nanoparticle is characteristic of nZVI and its magnetic behaviour.[6]

The powder XRD of C-nZVI showed a major reflection at $2\theta = 44.6^\circ$ (index 110) indicating the presence of Fe^0 on the cellulose surface (Fig. 1B).[18] Further, the reflections at $2\theta = 15.0$, 22.7 and 35.0° suggest the existence of cellulose in cellulose-I crystalline form.[19] Cellulose-I is the predominant crystalline form in MCC. Since adsorption process depends upon the surface area of the material, Brunauer–Emmett–Teller (BET) analysis of C-nZVI was carried out. The specific surface area of C-nZVI was found to be 9.55 $m^2\ g^{-1}$ (ESI Fig. S2†) which is significantly higher than MCC (1.3 $m^2\ g^{-1}$).[20] This could be accounted to the alkaline reducing agent induced pretreatment of cellulose leading to surface area increase under mechanical stirring condition.[21]

Further, the constituents of C-nZVI were established by XPS survey scan between 0–1000 eV (Fig. 1C). The binding energies corresponding to Fe1s and $Fe2p_{3/2}$ were observed at 107.4 and 714.4 eV, respectively. These binding energy peaks indicate the presence of zerovalent iron nanoparticles immobilized on cellulose.[22] The binding energy analysis showed C1s and O1s peak at 287 and 536.9 eV, respectively, which signifies the presence of cellulose. These binding energy peaks are attributed to polysaccharide moieties of cellulose.[23] The FTIR spectra of MCC and C-nZVI were carried out to understand the surface interaction between cellulose and nZVI (Fig. 1D). MCC is characterized by the presence of absorption bands at 3424, 2921, 1372, 1680, 1433, 1164, 1114, 1058 and 896 cm^{-1}. The absorption bands at 1164, 1114, 1058 and 896 cm^{-1} are characteristic of the pyranose ring structure of the monomer in cellulose.[23b] Upon immobilization of nZVI on MCC, narrowing of the absorption band at 3424 cm^{-1} was observed, which indicates the interaction of hydroxyl moieties of cellulose with nZVI in the material.[24] Further no significant change in the absorption band of C-nZVI was observed in comparison to MCC.

The stability of C-nZVI was studied by TGA and DTA behaviour (Fig. 1E and F). It was observed that MCC underwent thermal degradation in the temperature range of 300–350 °C, (upto 90% weight loss) while C-nZVI was degraded in two stages in the temperature range of 270–280 °C and 300–345 °C. The degradation of C-nZVI at lower temperature establishes its poor stability in comparison to MCC which is accounted to the exoergic oxidation of Fe^0 by cellulose present in the near vicinity. A part of C-nZVI degraded at higher temperature, which is due to the oxidation of charred carbon residues on the oxidized iron.[25]

C-nZVI was investigated for its adsorption efficiency and removal of Cr(VI) from aqueous solution. The conditions for Cr(VI) adsorption from aqueous solution were optimized in terms of pH, adsorbent dosage and equilibration time. The optimum conditions were observed to be pH 3, adsorbent dosage 100 mg L^{-1} and

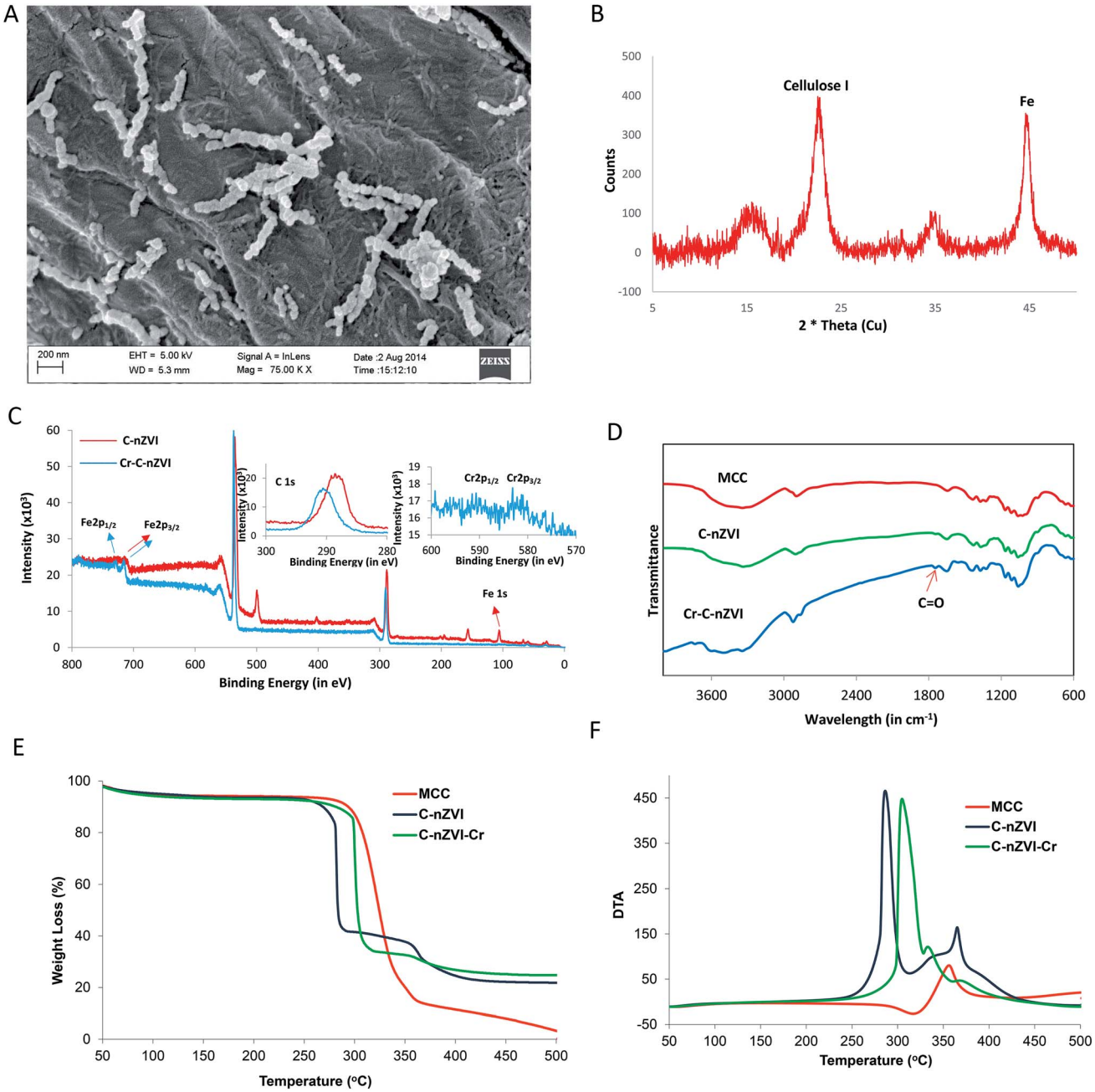

Fig. 1 [A] SEM image, [B] XRD pattern of C-nZVI, [C] XPS analysis of C-nZVI and Cr(VI) adsorbed C-nZVI. Inset Cr2p spectra of Cr(VI) adsorbed C-nZVI and C1s spectra of Cr(VI) adsorbed C-nZVI, [D] FTIR analysis of MCC, C-nZVI and Cr(VI) adsorbed C-nZVI, [E] TGA and [F] DTA.

equilibration time of 2 h (Fig. 2A–C). The maximum Cr(VI) removal occurred at pH 3 and the removal efficiency falls significantly upon increasing the pH.[18a,26] Equilibrium studies were carried out at pH 3, with an adsorbent dose at 100 mg L^{-1} and Cr(VI) concentration varying between 1–10 mg L^{-1}. The Cr(VI) uptake increased upto 10 mg L^{-1} Cr(VI) concentration (Fig. 2B). Non-linear Langmuir and Freundlich adsorption isotherm best fitted for the adsorption of Cr(VI) by C-nZVI signifying a monolayer adsorption behaviour of the material. The C-nZVI showed a maximum adsorption of 66.42 mg Cr(VI) per g of nZVI. Multilayered adsorption models non-linear curve fitting analysis for chromium adsorption on C-nZVI showed monolayer adsorption of chromium.[18a,27] Further adsorption kinetics of C-nZVI obeyed pseudo-second order kinetics with an equilibration period of 2 h (Fig. 2C). Similar pseudo-second order kinetics was observed for Cr(VI) adsorption by nZVI and immobilized nZVI (ESI Fig. S9†).[18a]

The maximum Cr(VI) adsorption was normalized for the iron content as cellulose did not show any affinity for Cr(VI) adsorption. Thus, the calculated adsorption was observed to be 562.8 mg Cr(VI) per g of Fe^0. Earlier studies by Jabeen *et al.*[18a] and Li *et al.*[28] on Cr(VI) adsorption by graphene and PVDF/PAA, respectively, were normalised for Cr(VI) adsorption. The

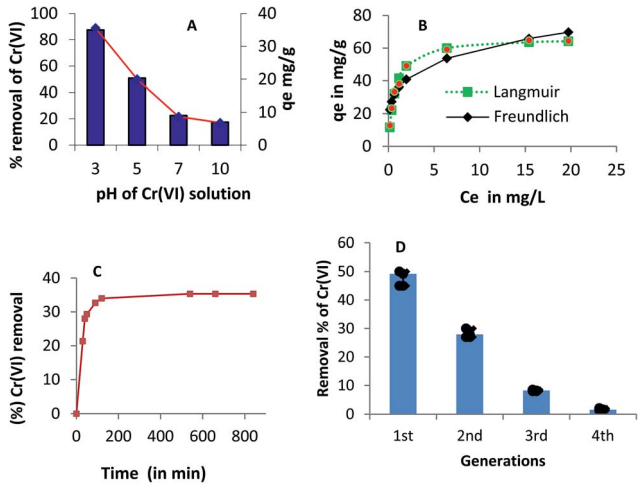

Fig. 2 Effect of [A] pH, [B] nonlinear adsorption isotherm, [C] contact time and [D] regeneration study of C-nZVI for chromium.

normalized Cr(VI) adsorption was found to be 172.3 and 181 mg g^{-1} of Fe^0 using nZVI stabilized/immobilized with graphene[18a] and PVDF/PAA,[28] respectively. Compared with these materials immobilized with nZVI, C-nZVI showed unusually high atom efficient adsorption of Cr(VI) from aqueous solution. Further when the rate constant for the adsorption of Cr(VI) by C-nZVI was compared with similar studies on graphene[18a] and montmorillonitrile,[29] a significantly lowering in the rate constant (1.7×10^{-5} min^{-1}) was observed (ESI Section 11†). In the regeneration study of Cr(VI) using C-nZVI, four successive generation of Cr(VI) reduction was found. The result showed 49.38% of Cr(VI) removal in the first generation which was reduced to 1.40% in fourth generation (Fig. 2D).

Further to investigate the unusual activity of C-nZVI for chromium adsorption, chromium adsorbed material was compared for SEM, XPS FTIR and TGA behaviour. SEM image of chromium adsorbed C-nZVI showed the presence of scattered iron material over the cellulose surface. EDX analysis established the presence of chromium on the surface. Adsorption of chromium onto C-nZVI, showed a clear shift in the FTIR absorption bands (Fig. 1D). Upon adsorption of Cr(VI), the band broadening in the region of 3000–3400 cm^{-1} occurs, which corresponds to the weakening of hydrogen bonding between nZVI and MCC in C-nZVI. This reflects the change in the surface morphology of the iron nanoparticle. Further a new absorption band was observed at 1734 cm^{-1} in case of chromium adsorbed C-nZVI which is accounted to the carbonyl moiety. This carbonyl functional group indicates the formation of cellulose dialdehyde.[30] This was further confirmed from the TG/DT, XPS and CHN analysis of the chromium adsorbed C-nZVI (Fig. 1C–E). The TG analysis of the Cr adsorbed sample showed that the thermal degradation of cellulose occurs in a narrow temperature range of 280–290 °C, which is significantly similar to the TG pattern of cellulose dialdehyde.[25] There is no significant change observed upto 500 °C which indicates that iron is in the completely oxidized form. The XPS spectrum for Cr adsorbed C-nZVI was carried out to understand the mechanism of adsorption (Fig. 3). The binding energy analysis revealed a C1s peak at 290 eV, which is found to drift in comparison to that reported by Sun *et al.* (2007).[31] The O1s binding energy peak is observed with a considerable shift at 536 eV, which is assigned to the cellulose hydroxyl moieties. The XPS peaks of $Fe2p_{3/2}$ and $Fe2p_{1/2}$ appear at 715.8 eV and 728.6 eV, respectively, which is again shifted from that of C-nZVI. This

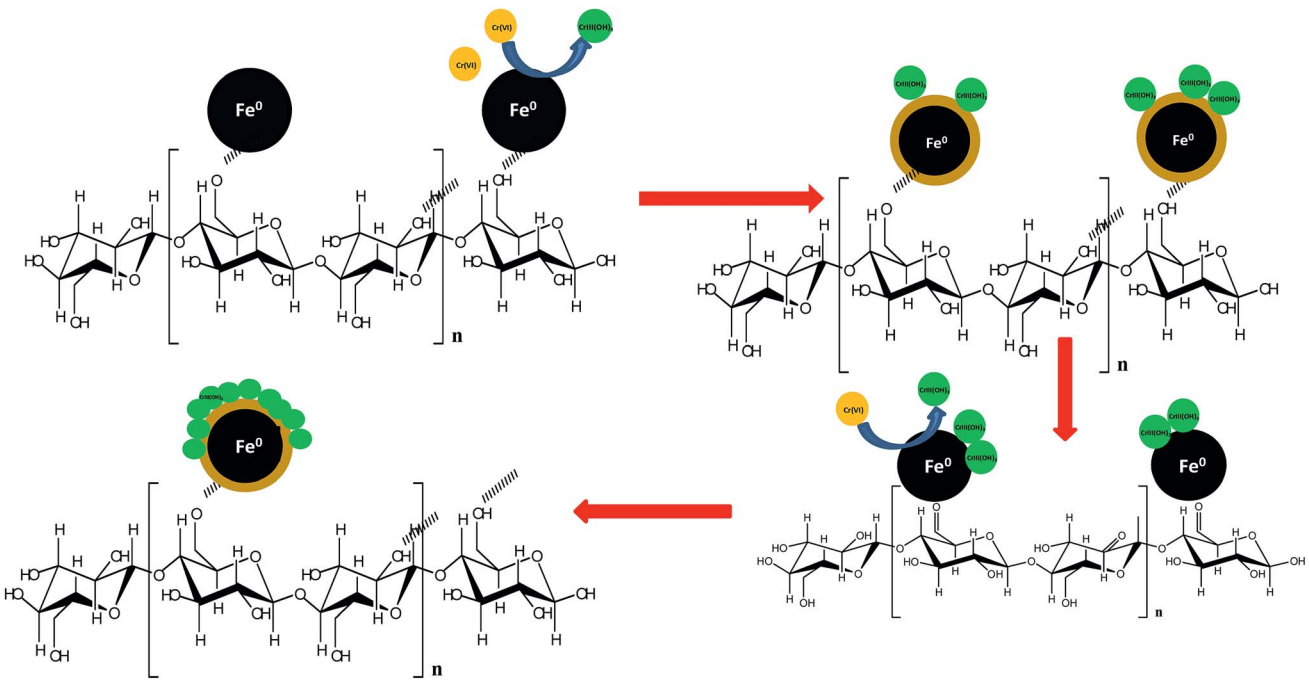

Fig. 3 Mechanism for the adsorption of Cr(VI) by C-nZVI.

suggests the presence of oxidized iron and the absence of nanozerovalent iron in the material. Weak $Cr2p_{1/2}$ and $Cr2p_{3/2}$ binding energy peaks were observed at 583.1 and 590.5 eV, respectively, confirms the presence of $Cr(III)OH_3$ adsorbed on the surface of nanomaterial.[27] This result corroborate the reduction of Cr(VI) to Cr(III) on the surface of nZVI, which simultaneously gets oxidizes to Fe(III) oxide.[27] The formation of dialdehyde was confirmed further by CHN analysis of oxime derivatized[32] C-nZVI, Cr(VI) adsorbed C-nZVI and Fe(III) treated MCC, the nitrogen content were found to be 0, 0.702 and 1.24%, respectively. This further indicates the absence of oxidation in C-nZVI but a significant aldehyde content was observed in other materials. Based on the results 1 : 24 and 1 : 13 glucose units were oxidized in case of Cr(VI) adsorbed C-nZVI and Fe(III) treated MCC, respectively. This suggests that Fe(III) has the tendency to oxidize MCC surface, which is formed during Cr(VI) adsorption, as evident from XPS studies. Further, the lesser extent of oxidation in Cr(VI) adsorbed C-nZVI in comparison to Fe(III) treated MCC suggests a localized oxidation by the iron oxide on the surface of Cr(VI) adsorbed C-nZVI sample.[30]

Based on the above results, the proposed mechanism of the sorption of C-nZVI is depicted in Fig. 3. nZVI adsorbs Cr(VI) by reductive sorption with oxidation of Fe^0 to Fe(III).[6a,27] The Fe(III) is reduced back and regenerated to Fe^0 by *in situ* oxidation of cellulose to cellulose dialdehyde. The regenerated iron further adsorbs chromium from the solution resulting in the atom efficient adsorption of Cr(VI) by Fe^0 in C-nZVI.

Thus in summary, a novel reductive adsorbent based on the immobilization of nZVI on cellulose has been studied. An atom efficient Cr(VI) removal by reductive sorption on nZVI was achieved. The efficiency of nZVI is accounted to *in situ* recycling of nZVI by oxidation of cellulose to cellulose dialdehyde in the vicinity of the nanoparticle.

Acknowledgements

Dr J. N. Babu is thankful to DST-SERB, New Delhi for providing financial assistance under DST fast track Young Scientist Programme (Ref. No. 240/2010). The authors' acknowledgement support by Central University of Punjab, Bathinda, India for research facility, Central Instrumentation Facility and scholarships, UGC-DAE Consortium, Kalpakkam Node for XPS analysis and IIT Ropar for XRD.

References

1 (*a*) M. Gheju, *Water, Air, Soil Pollut.*, 2011, **222**, 103–148; (*b*) C. Noubactep, S. Care and R. Crane, *Water, Air, Soil Pollut.*, 2012, **223**, 1363–1382; (*c*) A. D. Henderson and A. H. Demond, *Environ. Eng. Sci.*, 2007, **24**, 401–423; (*d*) S. Bilardi, P. S. Calabro, S. Care, N. Moraci and C. Noubactep, *Clean: Soil, Air, Water*, 2013, **41**, 835–843; (*e*) C. Noubactep, *Clean: Soil, Air, Water*, 2013, **41**, 702–710.

2 (*a*) B. I. Kharisov, H. R. Dias, O. V. Kharissova, V. M. Jimenez-Perez, B. O. Perez and B. M. Flores, *RSC Adv.*, 2012, **2**, 9325–9358; (*b*) W. Yan, H. L. Lien, B. E. Koel and W. X. Zhang, *Environ. Sci.: Processes Impacts*, 2013, **15**, 63–77; (*c*) W. X. Zhang and D. W. Elliott, *Remed. J.*, 2006, **16**, 7–21; (*d*) B. Pan and B. Xing, *Eur. J. Soil Sci.*, 2012, **63**, 437–456; (*e*) M. Otto, M. Floyd and S. Bajpai, *Remed. J.*, 2008, **19**, 99–108; (*f*) R. A. Crane and T. B. Scott, *J. Hazard. Mater.*, 2012, **211–212**, 112–125; (*g*) R. Naidu, *Water, Air, Soil Pollut.*, 2013, **224**, 1–11.

3 (*a*) M. M. Khin, A. S. Nair, V. J. Babu, R. Murugan and S. Ramakrishna, *Energy Environ. Sci.*, 2012, **5**, 8075–8109; (*b*) S. Zhou, Y. Li, J. Chen, Z. Liu, Z. Wang and P. Na, *RSC Adv.*, 2014, **4**, 50699–50707; (*c*) B. I. Kharisov, H. R. Dias, O. V. Kharissova, A. Vazquez, Y. Pena and I. Gomez, *RSC Adv.*, 2014, **4**, 45354–45381; (*d*) S. Li, W. Wang, W. Yan and W. X. Zhang, *Environ. Sci.: Processes Impacts*, 2014, **16**, 524–533; (*e*) L. Alidokht, A. R. Khataee, A. Reyhanitabar and S. Oustan, *Clean: Soil, Air, Water*, 2011, **39**, 633–640; (*f*) P. Huang, Z. Ye, W. Xie, Q. Chen, J. Li, Z. Xu and M. Yao, *Water Res.*, 2013, **47**, 4050–4058; (*g*) G. Sheng, X. Shao, Y. Li, J. Li, H. Dong, W. Cheng, X. Gao and Y. Huang, *J. Phys. Chem. A*, 2014, **118**, 2952–2958; (*h*) X. Lv, X. Xue, G. Jiang, D. Wu, T. Sheng, H. Zhou and X. Xu, *J. Colloid Interface Sci.*, 2014, **417**, 51–59.

4 (*a*) W. F. Chen, L. Pan, L. F. Chen, Q. Wang and C. C. Yan, *RSC Adv.*, 2014, **4**, 46689–46696; (*b*) L. Wang, S. Q. Ni, C. Guo and Y. Qian, *J. Mater. Chem. A*, 2013, **1**, 6379–6387; (*c*) Y. C Lee, C. W. Kim, J. Y. Lee, H. J. Shin and J. W. Yang, *Desalin. Water Treat.*, 2009, **10**, 33–38; (*d*) Y. Zhuang, S. Ahn, A. L. Seyfferth, Y. Masue-Slowey, S. Fendorf and R. G. Luthy, *Environ. Sci. Technol.*, 2011, **45**, 4896–4903; (*e*) Y. Zhuang, S. Ahn and R. G. Luthy, *Environ. Sci. Technol.*, 2010, **44**, 8236–8242.

5 (*a*) Y. H. Hwang, D. G. Kim and H. S. Shin, *J. Hazard. Mater.*, 2011, **185**, 1513–1521; (*b*) D. Sparis, C. Mystrioti, A. Xenidis and N. Papassiopi, *Desalin. Water Treat.*, 2013, **51**, 2926–2933.

6 (*a*) A. Liu, J. Liu, B. Pan and W. X. Zhang, *RSC Adv.*, 2014, **4**, 57377–57382; (*b*) Y. Xie and D. M. Cwiertny, *Environ. Sci. Technol.*, 2012, **46**, 8365–8373; (*c*) S. M. Ponder, J. G. Darab and T. E. Mallouk, *Environ. Sci. Technol.*, 2000, **34**, 2564–2569; (*d*) H. S. Kim, J. Y. Ahn, K. Y. Hwang, I. K. Kim and I. Hwang, *Environ. Sci. Technol.*, 2010, **44**, 1760–1766.

7 (*a*) J. Trujillo-Reyes, J. R. Peralta-Videa and J. L. Gardea-Torresdey, *J. Hazard. Mater.*, 2014, **280**, 487–503; (*b*) G. Sheng, X. Shao, Y. Li, J. Li, H. Dong, W. Cheng and Y. Huang, *J. Mater. Chem. A*, 2014, **118**, 2952–2958; (*c*) S. Krajangpan, H. Kalita, B. J. Chisholm and A. N. Bezbaruah, *Environ. Sci. Technol.*, 2012, **46**, 10130–10136; (*d*) I. Dror, O. M. Jacov, A. Cortis and B. Berkowitz, *ACS Appl. Mater. Interfaces*, 2012, **4**, 3416–3423.

8 L. Alidokht, A. R. Khataee, A. Reyhanitabar and S. Oustan, *Desalination*, 2011, **270**, 105–110.

9 (*a*) N. Horzum, M. M. Demir, M. Nairat and T. Shahwan, *RSC Adv.*, 2013, **3**, 7828–7837; (*b*) Y. Zhou, B. Gao, A. R. Zimmerman, H. Chen, M. Zhang and X. Cao, *Bioresour. Technol.*, 2014, **152**, 538–542.

10 (*a*) S. Luo, T. Lu, L. Peng, J. Shao, Q. Zeng and J. D. Gu, *J. Mater. Chem. A*, 2014, **2**, 15463–15472; (*b*) N. Bezbaruah, S. Krajangpan, B. J. Chisholm, E. Khan and J. J. E. Bermudez, *J. Hazard. Mater.*, 2009, **166**, 1339–1343.

11 (*a*) J. Fatisson, S. Ghoshal and N. Tufenkji, *Langmuir*, 2010, **26**, 12832–12840; (*b*) R. Singh, V. Misra and R. P. Singh, *J. Nanopart. Res.*, 2011, **13**, 4063–4073.

12 (*a*) J. Shokri and K. Adibkia, Application of Cellulose and Cellulose Derivatives in Pharmaceutical Industries in Cellulose - Medical, *Pharmaceutical and Electronic Applications*, ed. T. van de Ven and L. Godbout, 2013, pp. 47–56, http://www.intechopen.com/books/cellulose-medical-pharmaceutical-and-electronic-applications/application-of-cellulose-and-cellulose-derivatives-in-pharmaceutical-industries; (*b*) D. P. Ho, H. H. Ngo and W. Guo, *Bioresour. Technol.*, 2014, **169**, 742–749.

13 J. Cai, S. Kimura, M. Wada and S. Kuga, *Biomacromolecules*, 2009, **10**, 87–94.

14 J. He, T. Kunitake and A. Nakao, *Chem. Mater.*, 2003, **15**, 4401–4406.

15 (*a*) K. K. R. Datta, E. Petala, K. J. Datta, J. A. Perman, J. Tucek, P. Bartak, M. Otyepka, G. Zoppellaro and R. Zboril, *Chem. Commun.*, 2014, **50**, 15673–15676; (*b*) S. Zhou, D. Wang, H.-Y. Sun, J. Chen, S. Wu and P. Na, *Water, Air, Soil Pollut.*, 2014, **225**, 1945.

16 APHA, *Standard methods for the examination of water and wastewater*, American Public Health Association, Washington, DC, 21st edn, 2005, pp. 3–68.

17 E. Harvey Jr, J. A. Smart and E. S. Amis, *Anal. Chem.*, 1955, **27**, 26–29.

18 (*a*) H. Jabeen, V. Chandra, S. Jung, J. W. Lee, K. S. Kim and S. B. Kim, *Nanoscale*, 2011, **9**, 3583–3585; (*b*) Y. Zhang, Y. Li and X. Zheng, *Sci. Total Environ.*, 2011, **409**, 625–630.

19 N. Terinte, R. Ibbett and K. C. Schuster, *Lenzinger Ber.*, 2011, **89**, 118–131.

20 S. Ardizzone, F. S. Dioguardi, T. Mussini, P. R. Mussini, S. Rondinini, B. Vercelli and A. Vertova, *Cellulose*, 1999, **6**, 57–69.

21 (*a*) J. Siroký, R. S. Blackburn, T. Bechtold, J. Taylor and P. White, *Carbohydr. Polym.*, 2011, **84**, 299–307; (*b*) V. B. Agbor, N. Cicek, R. Sparling, A. Berlin and D. B. Levin, *Biotechnol. Adv.*, 2011, **29**, 675–685.

22 J. E. Martin, A. A. Herzing, W. Yan, Q. X. Li, B. E. Koel, C. J. Kiely and W. X. Zhang, *Langmuir*, 2008, **24**, 4329–4334.

23 (*a*) L.-S. Johansson and J. M. Campbell, *Surf. Interface Anal.*, 2004, **36**, 1018–1022; (*b*) X. Yu, S. Tong, M. Ge, J. Zuo, C. Cao and W. Song, *J. Mater. Chem. A*, 2013, **1**, 959–965.

24 (*a*) F. Jones, J. B. Farrow and W. Van Bronswijk, *Langmuir*, 1998, **14**, 6512–6517; (*b*) F. He, D. Zhao, J. Liu and C. B. Roberts, *Ind. Eng. Chem. Res.*, 2007, **46**, 29–34.

25 U.-J. Kim and S. Kuga, *Thermochim. Acta*, 2001, **369**, 79–85.

26 L. N. Shi, X. Zhang and Z. L. Chen, *Water Res.*, 2011, **45**, 886–892.

27 (*a*) X. Q. Li, J. Cao and X. W. Zhang, *Ind. Eng. Chem. Res.*, 2008, **47**, 2131–2139; (*b*) X. Lv, J. Xu, G. Jiang, J. Tang and X. Xu, *J. Colloid Interface Sci.*, 2012, **369**, 460–469.

28 S. Li, T. Li, Z. Xiu and Z. Jin, *J. Environ. Monit.*, 2010, **12**, 1153–1158.

29 P. Wu, S. Li, L. Ju, N. Zhu, J. Wu, P. Li and Z. Dang, *J. Hazard. Mater.*, 2012, **219**, 283–288.

30 U.-J. Kim, M. Wada and S. Kuga, *Carbohydr. Polym.*, 2004, **56**, 7–10.

31 Y. P. Sun, X. Q. Li, W. X. Zhang and H. P. Wang, *Colloids Surf., A*, 2007, **308**, 60–66.

32 S. Vicin, E. Princi, G. Luciano, E. Frnceschi, E. Pedemonte, D. Oldak, H. Kaczmarek and A. Sionkowska, *Thermochim. Acta*, 2004, **418**, 123–130.